

Motion-induced spin transfer

Daigo Oue^{1,2} and Mamoru Matsuo^{1,3,4,5}

¹*Kavli Institute for Theoretical Sciences, University of Chinese Academy of Sciences, Beijing, 100190, China.*

²*The Blackett Laboratory, Department of Physics, Imperial College London,
Prince Consort Road, Kensington, London SW7 2AZ, United Kingdom **

³*CAS Center for Excellence in Topological Quantum Computation,
University of Chinese Academy of Sciences, Beijing 100190, China*

⁴*Advanced Science Research Center, Japan Atomic Energy Agency, Tokai, 319-1195, Japan*

⁵*RIKEN Center for Emergent Matter Science (CEMS), Wako, Saitama 351-0198, Japan*

(Dated: October 13, 2021)

We propose a spin transport induced by inertial motion. Our system is composed of two host media and a narrow vacuum gap in between. One of the hosts is sliding at a constant speed relative to the other. This mechanical motion causes the Doppler effect that shifts the density of states and the nonequilibrium distribution function in the moving medium. Those shifts induce the difference in the distribution function between the two media and result in tunnelling spin current. The spin current is calculated from the Schwinger-Keldysh formalism with a spin tunnelling Hamiltonian. This scheme does not require either temperature difference, voltage or chemical potential.

Introduction.— Transport is a universal phenomenon in physics. Utilising electron, neutron, and photon transports in free space have provided high precision measurements such as microscopy and spectroscopy, which have played important roles not only in physics but also pioneered materials science, chemistry, and biology. Precisely guiding those excitations in media has enabled electrical and optical communications and information storage. Recent advances in condensed matter physics have realised not only the transport of a single quantum but also the manipulation of its properties.

In an emerging field called spintronics, manipulation of the spin angular momenta of electrons has been conducted in various ways. For example, spin tunnelling transport at the interface between a normal metal and a ferromagnetic insulator can be driven by microwave irradiation on the ferromagnetic side. This type of spin transports known as the spin pumping effect [1–5]. We proposed that visible light could also be used to drive spin transport at metallic interfaces [6–8]. There is another popular way to drive the spin tunnelling where they make use of the temperature difference between two media, the spin Seebeck effect [9–12]. In these schemes, the differences in the nonequilibrium distributions between the two media drove the spin transports.

Another interesting direction in spintronics is to use a mechanical degree of freedom for spin manipulation. Since spin is a kind of angular momenta, it can be manipulated by mechanical rotation in accordance with the angular momentum conservation. Indeed, Barnett, Einstein and de Haas experimentally showed that rigid-body rotation interacts with magnetic moment originating from the spin angular momenta of electrons [13, 14]. The mechanical manipulation of spin is demonstrated in a variety of systems, including micromechanical systems [15–18], microfluid systems [19–21], atomic nuclei [22, 23], and quark-gluon plasma [24]. These effects can

be comprehensively understood as consequences of the spin-rotation coupling [25, 26].

Although there are various studies on the spin transport and manipulation by mechanical motion as reviewed in Ref. [27], there is no study on the spin tunnelling transport driven by mechanical motion. In this work, we show spin tunnelling transport between two media can be induced by inertial motion. Our proposal is closely related to non-contact friction [28–30] because the forces are nothing but linear momentum transfers between moving media. The mechanical motion empowers the linear momenta to be transferred from one medium to the other. Here, we consider spin transfer between moving media instead of linear momentum transfer.

We consider two media separated by a very narrow gap (FIG. 1). Each medium hosts a magnon and

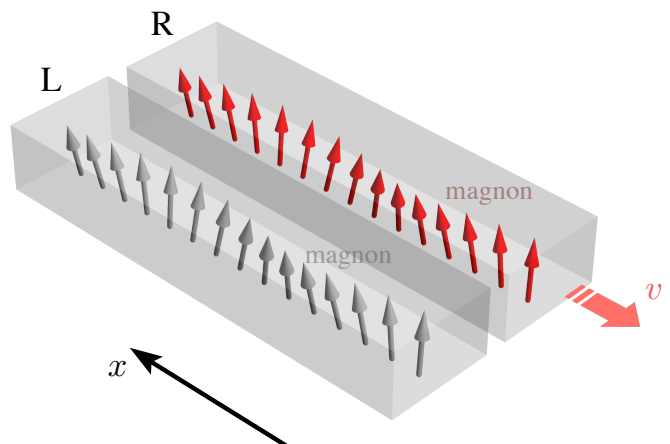


FIG. 1. The schematic image of the setup considered in this study. A very narrow gap separates two media hosting magnons. The right medium is moving in the $-x$ direction at a constant velocity v while the left medium stands still. Due to the Doppler effect, the dispersion relation of the magnon in the right medium observed in the laboratory frame is shifted.

is described by the following Hamiltonian within the Holstein–Primakoff approximation [31],

$$H_0 = E_0 + \sum_k \hbar \omega_k b_k^\dagger b_k, \quad (1)$$

where E_0 is the classical ground state energy of the medium, ω_k is the magnon dispersion relation, and we have introduced bosonic creation and annihilation operators.

The two media is interacting via the following tunnelling Hamiltonian,

$$H_{\text{int}} = \sum_k H_{\text{ex}} b_{Rk} b_{Lk}^\dagger + \text{H.c.} \quad (2)$$

where H_{ex} is a coupling strength, and the subscripts L and R specifies the medium. Although we assume the coupling strength H_{ex} is constant for simplicity in this study, it could be dependent on the wavenumber k .

Spin current induced by inertial motion.—Let us consider the change of the spin on the left medium in the interaction picture, we can obtain

$$\frac{\partial}{\partial t} \sum_k \langle S_k^z(t) \rangle = - \sum_k 2H_{\text{ex}} \text{Im} \langle b_{Rk}(t) b_{Lk}^\dagger(t) \rangle, \quad (3)$$

where $S_k^z = S - b_{Lk}^\dagger b_{Lk}$ is the z component of the spin in the left medium, and $\langle \dots \rangle$ denotes average with respect to the full Hamiltonian. Let us define the spin current flowing into the left medium at $t = t_1$,

$$\langle I_s(t_1) \rangle \equiv - \sum_k 2H_{\text{ex}} \text{Im} \langle b_{Rk}(t_1 - 0) b_{Lk}^\dagger(t_1) \rangle. \quad (4)$$

We shall omit \sum_k in the following where relevant.

Using the formal perturbative expansion (see, for example, Refs. [5, 32]), we can evaluate the spin current up to the second order in the coupling strength H_{ex} ,

$$\langle I_s(t_1) \rangle = \frac{2H_{\text{ex}}^2}{\hbar} \text{Re} \int_C \langle \mathcal{T}_C b_{Lk}^\dagger(t_1^-) b_{Lk}(t_2) \rangle_0 \times \langle \mathcal{T}_C b_{Rk}(t_1^+) b_{Rk}^\dagger(t_2) \rangle_0 dt_2, \quad (5)$$

where $\langle \dots \rangle_0$ is average with respect to the unperturbed Hamiltonian, and \mathcal{T}_C is the time-ordering operator on the Schwinger–Keldysh contour composed of a forward branch C_+ and backward one C_- (see FIG. 2). Note that t^\pm is times on the forward and backward branches.

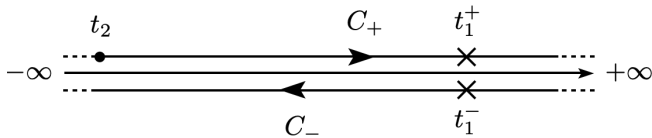


FIG. 2. Schwinger–Keldysh contour composed of forward and backward branches C_\pm .

Here, we introduce nonequilibrium Green’s function,

$$\chi_k(t_1, t_2) := \frac{1}{i\hbar} \langle \mathcal{T}_C b_k(t_1) b_k^\dagger(t_2) \rangle_0, \quad (6)$$

whose lesser and greater components read

$$\chi_{k;12}^< := \chi_k(t_1^+, t_2^-) = \frac{-i}{\hbar} \langle b_k^\dagger(t_2) b_k(t_1) \rangle_0, \quad (7)$$

$$\chi_{k;12}^> := \chi_k(t_1^-, t_2^+) = \frac{-i}{\hbar} \langle b_k(t_1) b_k^\dagger(t_2) \rangle_0. \quad (8)$$

We can write the chronologically ordered and anti-chronologically ordered components in terms of the lesser and greater components (7, 8),

$$\chi_{k;12}^{++} := \theta(t_1 - t_2) \chi_{k;12}^> + \theta(t_2 - t_1) \chi_{k;12}^<, \quad (9)$$

$$\chi_{k;12}^{--} := \theta(t_1 - t_2) \chi_{k;12}^< + \theta(t_2 - t_1) \chi_{k;12}^>, \quad (10)$$

where θ denotes the Heaviside unit step function.

Splitting the contour C into the forward and backwards parts, we can write the real time representation,

$$\frac{\langle I_s(t_1) \rangle}{2\hbar H_{\text{ex}}^2} = - \text{Re} \int \left(\chi_{Rk;12}^{\Re} \chi_{Lk;21}^< + \chi_{Rk;12}^< \chi_{Lk;21}^{\Re} \right) dt_2, \quad (11)$$

where we have defined the retarded and advanced components,

$$\chi_{k;12}^{\Re} := \frac{-i}{\hbar} \theta(t_1 - t_2) \langle [b_k(t_1), b_k^\dagger(t_2)] \rangle_0 = \chi_{k;12}^{++} - \chi_{k;12}^<, \quad (12)$$

$$\chi_{k;12}^{\Im} := \frac{+i}{\hbar} \theta(t_2 - t_1) \langle [b_k(t_1), b_k^\dagger(t_2)] \rangle_0 = \chi_{k;12}^< - \chi_{k;12}^{--}, \quad (13)$$

which is nothing but the dynamical (magnetic) susceptibility of the medium. Note that the square brackets denotes the commutation relation here, i.e. $[\bullet, \circ] = \bullet \circ - \circ \bullet$.

In the steady-state, Green’s functions depend only on the time difference, e.g.

$$\chi_{k;12}^{\Re} = \frac{1}{2\pi} \int \chi_{k\omega}^{\Re} e^{-i\omega(t_1-t_2)} d\omega. \quad (14)$$

Thus, working on the frequency domain, we can simplify the integral (11) in the steady state,

$$\langle I_s^{\text{ss}} \rangle = \frac{4H_{\text{ex}}^2}{2\pi} \sum_{k>0} \int \Delta j_s^{\text{ss}}(k, \omega) d\omega, \quad (15)$$

$$j_s^{\text{ss}}(k, \omega) = \hbar \text{Im} \chi_{Lk\omega}^{\Re} \text{Im} \chi_{Rk\omega}^{\Re} \delta n_k. \quad (16)$$

Here, we have symmetrised the integrand with respect to the wavenumber, $\Delta j_s^{\text{ss}}(k, \omega) = j_s^{\text{ss}}(k, \omega) + j_s^{\text{ss}}(-k, \omega)$, and defined the distribution difference between the two media, $\delta n_k := n_b(\omega_{Lk}) - n_b(\omega_{Rk})$, where n_b denotes the Bose distribution function, and $\omega_{L(R)k}$ the magnon dispersion in the left (right) medium. Note that we have used the

Kadanoff–Baym ansatz, i.e. $\chi_{k\omega}^< = 2in_b(\omega_k) \text{Im} \chi_{k\omega}^{\mathfrak{R}}$, in order to get Eq. (15).

That is the formula we use to evaluate the spin current flowing between the two media. The integrand $\Delta j_s^{\text{ss}}(k, \omega)$ is composed of (i) the products of magnon spectra $\text{Im} \chi_{Lk\omega}^{\mathfrak{R}} \text{Im} \chi_{Rk\omega}^{\mathfrak{R}}$ and (ii) the distribution difference δn_k . This implies large spectral overlap and large population differences between the two media drive large spin currents.

In our setup, the inertial motion of the right medium is the key to generate a finite population difference. To consider the effects of inertial motion, we shall define the physical quantities in the co-moving frame and go back to the laboratory frame. In the nonrelativistic regime ($|v/c| \ll 1$), the Lorentz boost can be safely approximated by the Galilean boost, which we use to go back to the laboratory frame,

$$\begin{cases} t \rightarrow t, \\ x \rightarrow x - vt. \end{cases} \quad (17)$$

Applying the Galilean boost to a function $\psi(x)$, we have

$$\psi(x) = \frac{1}{2\pi} \iint \psi_{k\omega} e^{i(k \cdot x - \omega t)} dk d\omega, \quad (18)$$

$$\rightarrow \frac{1}{2\pi} \iint \psi_{k, \omega + v \cdot k} e^{i(k \cdot x - \omega t)} dk d\omega. \quad (19)$$

This implies that the Galilean boost (17) induces the Doppler effect, i.e. the spectra and hence the dispersion relations in moving media are shifted ($\omega_k \rightarrow \omega_k - v \cdot k$).

In our case, the spectrum and the distribution function of magnons in the right medium are shifted,

$$\begin{cases} \text{Im} \chi_{Rk\omega}^{\mathfrak{R}} \rightarrow \text{Im} \chi_{Rk, \omega + v \cdot k}^{\mathfrak{R}}, \\ n_b(\omega_{Rk}) \rightarrow n_b(\omega_{Rk} - v \cdot k). \end{cases} \quad (20)$$

When the two media are made of the same material, we substitute

$$\begin{cases} \text{Im} \chi_{Lk\omega}^{\mathfrak{R}} = \text{Im} \chi_{k\omega}^{\mathfrak{R}}, \\ \text{Im} \chi_{Rk\omega}^{\mathfrak{R}} = \text{Im} \chi_{k, \omega + v \cdot k}^{\mathfrak{R}}, \\ \delta n_k = n_b(\omega_k) - n_b(\omega_k - v \cdot k). \end{cases} \quad (21)$$

From the expression δn_k , we can immediately find that there is no spin current if the right medium is not moving ($v = 0$) In the following, we assume a simple parabolic dispersion for the magnon, $\omega_k = Dk^2 + \omega_0$, where $\omega_0 = \gamma B$ is the Zeeman energy. The retarded component of the magnon Green's function can be given in the frequency domain,

$$\chi_{k\omega}^{\mathfrak{R}} = \frac{1/\hbar}{\omega - \omega_k + i\Gamma}, \quad (22)$$

where Γ is spectral broadening, for example, due to surface roughness and impurity scattering.

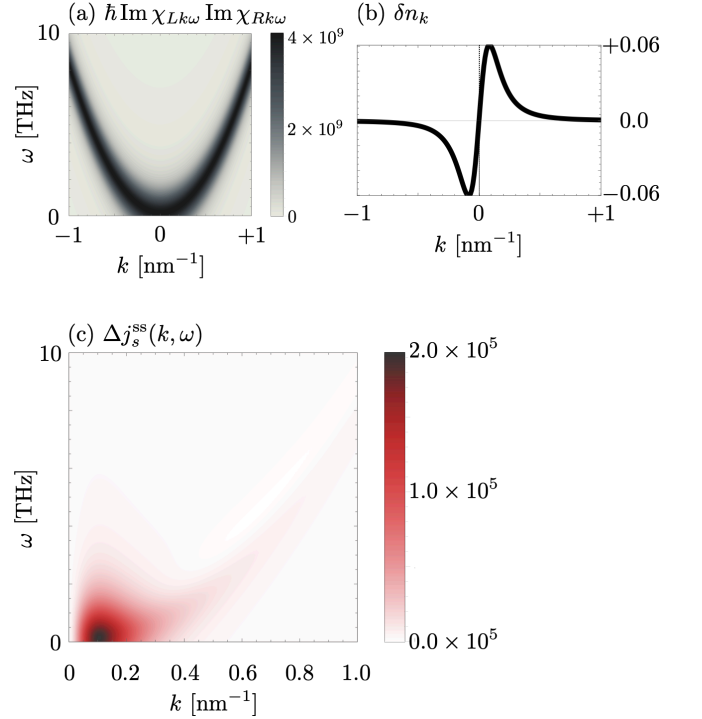


FIG. 3. (a) the spectral overlap of magnons in left and right media $\text{Im} \chi_{Lk\omega}^{\mathfrak{R}} \text{Im} \chi_{Rk\omega}^{\mathfrak{R}}$. (b) magnon distribution difference between left and right media δn_k . (c) the integrand $\Delta j_s^{\text{ss}}(k, \omega)$ that yields the tunneling spin current. We set the spectral broadening due to disorder $\Gamma = 1$ [meV] ≈ 0.24 [THz], the velocity of the right medium $v = 1$ [$\text{m} \cdot \text{s}^{-1}$], the static magnetic field $B = 1$ [T] and $D = 532$ [$\text{meV} \cdot \text{\AA}^2$] in accordance with Ref. [33],

In FIG. 3 (c), the integrand $\Delta j_s^{\text{ss}}(k, \omega)$ in the spin current formula (15) is plotted. Since the Doppler shift $\Delta \omega_k = v \cdot k$ is smallest when $k = 0$, the spectral overlap $\text{Im} \chi_{Lk\omega}^{\mathfrak{R}} \text{Im} \chi_{Rk\omega}^{\mathfrak{R}}$ becomes large in the low frequency region [see FIG. 3 (a)]. We can see that the amount of the distribution difference δn_k is large in low wavenumber region [see FIG. 3 (b)]. This implies the dominant contribution to the steady-state spin current $\langle I_s^{\text{ss}} \rangle$ comes from that region and justifies introducing cutoff frequency and wavenumber when evaluating the integral (15) in numerics.

Numerically integrating the spin current formula (15), we can obtain FIGs. 4 and 5. In order to obtain those figures, we substituted a far smaller number into the coupling strength than the magnon energy ($H_{\text{ex}} \ll \hbar \omega_0 < \hbar \omega_k$), and thus, we can safely adopt the perturbative evaluation of the spin current.

We have plotted the spin current $\langle I_s^{\text{ss}} \rangle$ as a function of the right medium velocity v for three different temperatures in FIG. 4. As the velocity v is larger, the Doppler shift $\Delta \omega = v \cdot k$ and hence the distribution difference δn_k increases. This is why the spin current increases with the velocity of the right medium. We can fit the spin current

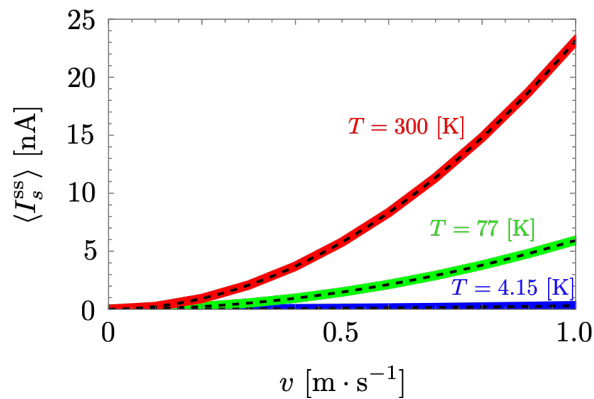


FIG. 4. Spin current at the steady state $\langle I_s^{ss} \rangle$ as a function of the velocity of the right medium v . Blue, gray, and red curves are the spin currents at liquid helium, liquid nitrogen, and room temperatures, ($T = 4.15, 77, 300$ [K]). We set the coupling strength $H_{\text{ex}} = 1$ [GHz] ≈ 50 [meV], which is far smaller compared with the magnon frequency (i.e. $H_{\text{ex}} \ll \hbar\omega_k$). The other parameters are the same as the previous figure. Each curve can be fitted by a parabolic function (black dashed curve). This implies the motion-induced spin transfer is the second-order effect.

by a parabolic function. This reflects the fact that the leading term of the motion-induced spin current is the second order, i.e. $\langle I_s^{ss} \rangle \propto H_{\text{ex}}^2$.

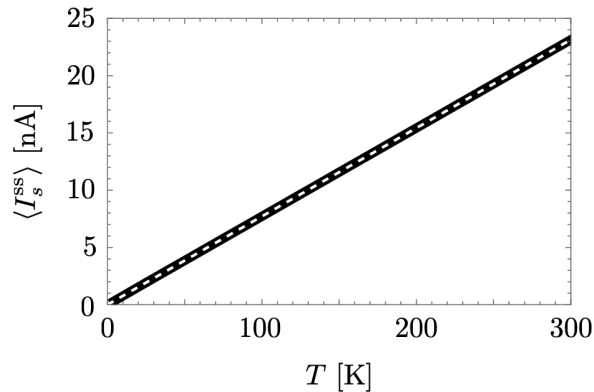


FIG. 5. Spin current at the steady state $\langle I_s^{ss} \rangle$ as a function of temperature T . Since the spin current can be fitted by a linear function (white dashed line), the motion-induced spin transfer is proportional to the temperature T . We set $v = 1$ [m · s⁻¹] and other parameters the same as the previous figures.

In FIG. 5, we show the temperature dependence of the spin current. The spin current can be linearly fitted (see the white line in the figure) and is proportional to the temperature T .

Conclusions.—In this Letter, we proposed motion-induced spin transfer between two media which host and can exchange magnons. One of the two media is moving at a constant velocity, and the inertial motion causes the Doppler effect. This results in the spectral shift of the

magnon spectrum and distribution function in the moving medium. According to our perturbative calculation within the Schwinger–Keldysh formalism, the difference in the magnon distribution between the two media drives the spin transfer from the moving one to the other.

As for the possibility of the experimental verification of our proposal, we could use state-of-the-art inverse spin Hall measurement used, for example, in Ref. [19], which can detect an electric signal of the order of 1 nV.

Our proposal will open a new door to spin manipulation by inertial motion.

D.O and M.M. deeply thank Yuya Ominato for fruitful discussion on the nonequilibrium Green’s function method. D.O. is funded by the President’s PhD Scholarships at Imperial College London. This work is partially supported by the Priority Program of Chinese Academy of Sciences, Grant No. XDB28000000 and Grant-in-Aid for Scientific Research B (20H01863) from MEXT, Japan.

* daigo.oue@gmail.com

- [1] R. Silsbee, A. Janossy, and P. Monod, Coupling between ferromagnetic and conduction-spin-resonance modes at a ferromagnetic–normal-metal interface, *Physical Review B* **19**, 4382 (1979).
- [2] Y. Tserkovnyak, A. Brataas, and G. E. Bauer, Enhanced Gilbert damping in thin ferromagnetic films, *Physical review letters* **88**, 117601 (2002).
- [3] I. Žutić, J. Fabian, and S. D. Sarma, Spintronics: Fundamentals and applications, *Reviews of modern physics* **76**, 323 (2004).
- [4] Y. Ohnuma, H. Adachi, E. Saitoh, and S. Maekawa, Enhanced dc spin pumping into a fluctuating ferromagnet near t c, *Physical Review B* **89**, 174417 (2014).
- [5] T. Kato, Y. Ohnuma, M. Matsuo, J. Rech, T. Jonckheere, and T. Martin, Microscopic theory of spin transport at the interface between a superconductor and a ferromagnetic insulator, *Physical Review B* **99**, 144411 (2019).
- [6] D. Oue and M. Matsuo, Electron spin transport driven by surface plasmon polaritons, *Physical Review B* **101**, 161404(R) (2020).
- [7] D. Oue and M. Matsuo, Effects of surface plasmons on spin currents in a thin film system, *New Journal of Physics* **22**, 033040 (2020).
- [8] D. Oue and M. Matsuo, Optically induced electron spin currents in the Kretschmann configuration, *Physical Review B* **102**, 125431 (2020).
- [9] K. Uchida, S. Takahashi, K. Harii, J. Ieda, W. Koshibae, K. Ando, S. Maekawa, and E. Saitoh, Observation of the spin seebeck effect, *Nature* **455**, 778 (2008).
- [10] K.-i. Uchida, J. Xiao, H. Adachi, J.-i. Ohe, S. Takahashi, J. Ieda, T. Ota, Y. Kajiwara, H. Umezawa, H. Kawai, *et al.*, Spin seebeck insulator, *Nature materials* **9**, 894 (2010).
- [11] K.-i. Uchida, H. Adachi, T. Ota, H. Nakayama, S. Maekawa, and E. Saitoh, Observation of longitudinal spin-seebeck effect in magnetic insulators, *Applied Physics Letters* **97**, 172505 (2010).

- [12] H. Adachi, J.-i. Ohe, S. Takahashi, and S. Maekawa, Linear-response theory of spin seebeck effect in ferromagnetic insulators, *Physical Review B* **83**, 094410 (2011).
- [13] A. Einstein and W. De Haas, Experimental proof of the existence of Ampère's molecular currents, in *Proc. KNAW*, Vol. 18 I (1915) p. 696.
- [14] S. J. Barnett, Magnetization by rotation, *Physical Review* **6**, 239 (1915).
- [15] T. M. Wallis, J. Moreland, and P. Kabos, Einstein-de Haas effect in a nife film deposited on a microcantilever, *Applied physics letters* **89**, 122502 (2006).
- [16] G. Zolfagharkhani, A. Gaidarzhy, P. Degiovanni, S. Kettemann, P. Fulde, and P. Mohanty, Nanomechanical detection of itinerant electron spin flip, *Nature Nanotechnology* **3**, 720 (2008).
- [17] D. Kobayashi, T. Yoshikawa, M. Matsuo, R. Iguchi, S. Maekawa, E. Saitoh, and Y. Nozaki, Spin current generation using a surface acoustic wave generated via spin-rotation coupling, *Physical review Letters* **119**, 077202 (2017).
- [18] K. Harii, Y.-J. Seo, Y. Tsutsumi, H. Chudo, K. Oyanagi, M. Matsuo, Y. Shiomi, T. Ono, S. Maekawa, and E. Saitoh, Spin seebeck mechanical force, *Nature communications* **10**, 1 (2019).
- [19] R. Takahashi, M. Matsuo, M. Ono, K. Harii, H. Chudo, S. Okayasu, J. Ieda, S. Takahashi, S. Maekawa, and E. Saitoh, Spin hydrodynamic generation, *Nature Physics* **12**, 52 (2016).
- [20] H. T. Kazerooni, A. Thieme, J. Schumacher, and C. Cierpka, Electron spin-vorticity coupling in pipe flows at low and high reynolds number, *Physical Review Applied* **14**, 014002 (2020).
- [21] H. T. Kazerooni, G. Zinchenko, J. Schumacher, and C. Cierpka, Electrical voltage by electron spin-vorticity coupling in laminar ducts, *Physical Review Fluids* **6**, 043703 (2021).
- [22] H. Chudo, M. Ono, K. Harii, M. Matsuo, J. Ieda, R. Haruki, S. Okayasu, S. Maekawa, H. Yasuoka, and E. Saitoh, Observation of barnett fields in solids by nuclear magnetic resonance, *Applied Physics Express* **7**, 063004 (2014).
- [23] A. Wood, E. Lilette, Y. Fein, V. Perunicic, L. Hollenberg, R. Scholten, and A. Martin, Magnetic pseudo-fields in a rotating electron-nuclear spin system, *Nature Physics* **13**, 1070 (2017).
- [24] L. Adamczyk, J. Adkins, G. Agakishiev, M. Aggarwal, Z. Ahammed, N. Ajitanand, I. Alekseev, D. Anderson, R. Aoyama, A. Aparin, *et al.*, Global λ hyperon polarization in nuclear collisions, *Nature (London)* **548** (2017).
- [25] M. Matsuo, J. Ieda, K. Harii, E. Saitoh, and S. Maekawa, Mechanical generation of spin current by spin-rotation coupling, *Physical Review B* **87**, 180402 (2013).
- [26] M. Matsuo, Y. Ohnuma, and S. Maekawa, Theory of spin hydrodynamic generation, *Physical Review B* **96**, 020401 (2017).
- [27] M. Matsuo, E. Saitoh, and S. Maekawa, Spin-mechatronics, *Journal of the Physical Society of Japan* **86**, 011011 (2017).
- [28] K. Saitoh, K. Hayashi, Y. Shibayama, and K. Shira-hama, Gigantic maximum of nanoscale noncontact friction, *Physical review Letters* **105**, 236103 (2010).
- [29] J.-H. She and A. V. Balatsky, Noncontact friction and relaxational dynamics of surface defects, *Physical review Letters* **108**, 136101 (2012).
- [30] K. Milton, J. Høye, and I. Brevik, The reality of casimir friction, *Symmetry* **8**, 29 (2016).
- [31] T. Holstein and H. Primakoff, Field dependence of the intrinsic domain magnetization of a ferromagnet, *Physical Review* **58**, 1098 (1940).
- [32] M. Matsuo, Y. Ohnuma, T. Kato, and S. Maekawa, Spin current noise of the spin seebeck effect and spin pumping, *Physical review Letters* **120**, 037201 (2018).
- [33] A. J. Princep, R. A. Ewings, S. Ward, S. Tóth, C. Dubs, D. Prabhakaran, and A. T. Boothroyd, The full magnon spectrum of yttrium iron garnet, *npj Quantum Materials* **2**, 1 (2017).